Journal of Solid State Chemistry 182 (2009) 1408–1416

Contents lists available at ScienceDirect

Journal of Solid State Chemistry

journal homepage: www.elsevier.com/locate/jssc

Syntheses, topological analyses and photoelectric properties of Ag(I)/Cu(I) metal-organic frameworks based on a tetradentate imidazolate ligand ☆

Hua-Sen Weng [a,b], Jian-Di Lin [a,b], Xi-Fa Long [a], Zhi-Hua Li [a,b], Ping Lin [a], Shao-Wu Du [a,*]

[a] State Key Laboratory of Structural Chemistry, Fujian Institute of Research on the Structure of Matter, Chinese Academy of Sciences, Fuzhou, Fujian 350002, PR China
[b] Graduate University of Chinese Academy of Sciences, Beijing 100039, PR China

ARTICLE INFO

Article history:
Received 7 November 2008
Received in revised form
4 March 2009
Accepted 16 March 2009
Available online 26 March 2009

Keywords:
Coordination polymers
Tetradentate imidazolate ligand
Pseudohalide-bridging
Ferroelectric
Photoluminescent property
Topology analyses

ABSTRACT

A new tetradentate imidazolate ligand 1,1′,1″,1‴-(2,2′,4,4′,6,6′-hexamethylbiphenyl-3,3′,5,5′-tetrayl)tetrakis(methylene)(1H-imidazole) (L) and four Ag(I)/Cu(I) coordination polymers, namely $[(MCN)_3L]_n$ (**1**: $M=Ag$; **2**: $M=Cu$), and $[(MSCN)_2L]_n$ (**3**: $M=Ag$; **4**: $M=Cu$) are described. All four new coordination polymers were fully characterized by infrared spectroscopy, elemental analysis and single-crystal X-ray diffraction. Compound **1** features a 3D supramolecular framework constructed by 1D chains through inter-chain Ag–N(CN) and inter-layer Ag–N(L) weak interactions with an uninodal 6^6 topology. Complex **2** presents a 3D framework characterized by a tetranodal (3,4)-connected $(3\cdot4\cdot5\cdot10^2\cdot11)(3\cdot4\cdot5\cdot6\cdot7\cdot9)(3\cdot6\cdot7)(6\cdot10^2)$ topology. Complexes **3** and **4** are isostructural, and both have a 3D network of trinodal 4-connected $(4\cdot8^5)_2(4^2\cdot8^2\cdot10^2)(4^2\cdot8^4)_2$ topology. The luminescent properties for these compounds in the solid state as well as the possible ferroelectric behavior of **1** are discussed.

1. Introduction

There is growing interest in the design and synthesis of metal-organic coordination polymers not only for their intriguing aesthetic structures and topological features, but also for their potential properties as functional materials, and for the development of optical, magnetic and electronic devices [1–3]. One of the common strategies for the construction of metal-organic coordination polymers is the design of new types of organic bridging ligands, especially those containing N- or O-donor groups [4–8]. Recently, the imidazole-containing tectons have gained more interest as ligands to bridge metal ions in the construction of functional coordination polymers, because of their versatile ligand types and variational ligand conformations compared to the rigid N-donor ligands, such as 4,4′-bipyridyl and its analogs. In general, the flexibility of imidazolate ligands usually results in the formation of novel network topologies because their flexibility and conformational freedom allow for greater structural diversity [9–16]. For example, the utilization of multidentate imidazole-based ligands, of which bix (1,4-bis(imidazol-1-ylmethyl)-benzene) is an ubiquitous example, in combination with metal centers with varying geometries can give rise to a large number of structurally interesting coordination polymers, such as 1D linear or zig-zag-like chains [9], 2D square grids [10] or interwoven honeycombs [9], or 3D diamondoid frameworks [11]. In this field, however, much of the work has so far focused on bi, tri and hexadentate imidazolate ligands, and the coordination chemistry of tetradentate imidazolate ligands is surprisingly underdeveloped [17,18].

Moreover, silver(I) and copper(I) ions are good candidates as soft acids tending to coordinating to soft bases such as ligands containing sulfur and nitrogen atoms [19,20]. They are particularly well-suited cations not only because of their labile coordination modes with coordination numbers 2–5 but also because they are apt to form metal–metal interactions, which are propitious to control supramolecular architectures and dimensionality [21–23]. On the other hand, cyanide and thiocyanate are well-known bridging ligands for the construction of coordination polymers due to their ambidexterous character and considerably flexible coordination modes [24–26]. Though Ag(I)/Cu(I)X ($X=CN^-$ or SCN^-) coordination polymers containing bridging N-donor ligands are documented, most of them are those involving bitopic pyridyl (or imidazole)-based linkers and those with tri- or tetradentate N-donor ligands remain unexplored up to now [27–37].

Very recently, we have designed and synthesized a new tetradentate imidazolate ligand bis(3,5-bis((1H-imidazol-1-yl)-methyl)-2,4,6-trimethylphenyl)methane) and investigated its assembly reactions with Ag(I) complexes [17]. As a continuous work, in this study, a similar tetradentate imidazolate ligand L (Scheme 1) is prepared. The reactions of L with Ag(I)/Cu(I)X

☆ Dedicated to Prof. Xin-Tao Wu on the occasion of his 70th birthday.

* Corresponding author. Fax: +86 591 83709470.
E-mail address: swdu@fjirsm.ac.cn (S.-W. Du).

0022-4596/$ - see front matter © 2009 Elsevier Inc. All rights reserved.
doi:10.1016/j.jssc.2009.03.012

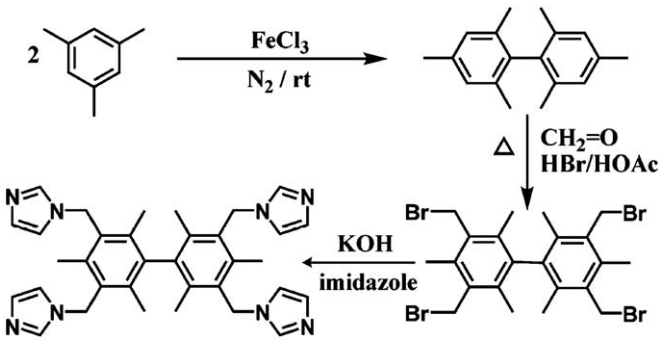

Scheme 1. Synthetic route of ligand.

($X = CN^-$ or SCN^-) afforded four new coordination polymers $[(MCN)_3L]_n$ (**1**: M = Ag; **2**: M = Cu) and $[(MSCN)_2L]_n$ (**3**: M = Ag; **4**: M = Cu). The crystal structures and topological analyses of these compounds, along with the investigation of their photoelectric properties, have been discussed.

2. Experimental

2.1. General

All commercially available chemicals are of reagent grade and were used as received. Bimesityl was prepared according to the literature method [38]. Elemental analysis was conducted on a Vario EL III elemental analyzer. ^{1}H NMR spectra were recorded on a Varian Unity-500 spectrometer, operating at 499.802 MHz. The FT-IR spectra were recorded from KBr pellets in the range 4000–400 cm^{-1} on a Nicolet Magna 750 FT-IR spectrophotometer. Fluorescent analyses were performed on an Edinburgh Instruments FL920 analyzer. The measurement of the polarization–voltage curves was carried out on a pellet of the powder sample with an aixACCT TF Analyzer 2000 system at room temperature, and the pellet (diameter of 6 mm and thickness of 0.6 mm) was sandwiched by silver electrodes and immerged in insulating oil while measuring. The frequency dependence of permittivity was measured on Agilent 4284A Precision LCR Meter at room temperature using the former sample. Powder X-ray diffraction patterns were recorded on a PANalytical X'pert Pro X-ray diffractometer with graphite-monochromatized Cu$K\alpha$ radiation ($\lambda = 1.542$ Å). Thermogravimetric experiments were performed using a TGA/SDTA851 instrument (heating rate of 15 °C min^{-1}, nitrogen stream).

2.2. Synthesis of 3,3′,5,5′-tetrakis(bromomethyl)-2,2′,4,4′,6,6′-hexamethylbiphenyl

The synthetic procedure was applied following the comparative method as described for tris(bromomethyl)mesitylene [39]. To a mixture of Bimesityl (4.9 g, 20 mmol), paraformaldehyde (2.8 g, 100 mmol), and 50 mL of glacial acetic acid was added 20 mL of a HBr/acetic acid solution (31 wt%) rapidly. The mixture was stirred for 12 h at 120 °C and then 100 mL of water was added. The white precipitate was filtered off, washed with water several times and dried in vacuum (yield: 95%). IR (cm^{-1}): 3413 (w), 2989 (w), 2917 (w), 1637 (w), 1616 (w), 1565 (w), 1448 (s), 1373 (m), 1235 (m), 1203 (vs), 1015 (w), 836 (s), 759 (w), 749 (w), 668 (w), 564 (s), 545 (s), 468 (m). Anal. calcd for $C_{22}H_{26}Br_4$ (610.06): C, 43.31; H, 4.30. Found: C, 43.27; H 4.38.

2.3. Synthesis of 1,1′,1″,1‴-(2,2′,4,4′,6,6′-hexamethylbiphenyl-3,3′,5,5′-tetrayl)tetrakis(methylene)(1H-imidazole) (L)

The synthetic procedure was applied following the comparative method as described for titb [40]. Imidazole (2.6 g, 40 mmol) and potassium hydroxide (10.0 g, 178 mmol) were dissolved in 100 mL of DMSO and the mixture was stirred for 2 h at room temperature, then 3,3′,5,5′-tetrakis(bromomethyl)-2,2′,4,4′,6,6′-hexamethylbiphenyl (6.0 g, 10 mmol) was added. After stirring for 2 days at room temperature, an equivalent volume of water was added to the mixture. The aqueous solution was extracted with chloroform (4 × 50 mL). The combined organic extracts were washed with water and dried over anhydrous sodium sulfate. Solvent was removed and excess diethyl ether was added to the residue. After standing overnight at −18 °C, the white powder was filtered, washed with diethyl ether and dried in vacuum (yield: 91%). IR (cm^{-1}): 3108 (m), 2983 (m), 1663 (m), 1511 (s), 1477 (m), 1391 (m), 1341 (w), 1274 (m), 1231 (vs), 1110 (s), 1078 (vs), 1023 (m), 916 (m), 846 (w), 820 (m), 744 (s), 664 (s) , 617 (m). ^{1}H NMR (CD_3Cl) δ 7.306 (s, 4H, H_{Im}), 7.054 (s, 4H, H_{Im}), 6.760 (s, 4H, H_{Im}), 5.250 (s, 8H, $-CH_2-$), 2.310 (s, 6H, $-CH_3$), 1.891 (s, 12H, $-CH_3$). Anal. Calcd for $C_{34}H_{38}N_8$ (558.73): C, 73.09; H, 6.85; N, 20.06. Found: C, 73.02; H, 6.97; N, 20.01.

2.4. Synthesis of the complexes *1–4*

2.4.1. $[(AgCN)_3L]_n$ (*1*)

A mixture of AgCN (33.5 mg, 0.25 mmol), L (46.5 mg, 0.1 mmol) and acetonitrile (2 mL) was sealed in a glass tube and heated at 120 °C for 2 days. After cooling to room temperature over 2 days, white prism crystals of **1** were obtained (68% yield based on Ag). Anal. calcd for $C_{37}H_{38}Ag_3N_{11}$ (960.39): C, 46.27; H, 3.99; N, 16.04. Found: C, 45.68; H, 3.32; N, 16.83. IR (cm^{-1}): 3134 (m), 3114 (m), 2922 (w), 2130 (m), 1611 (w), 1509 (s), 1476 (m), 1385 (s), 1234 (vs), 1111 (vs), 1081 (vs), 1022 (m), 827 (m), 759 (m), 737 (m), 656 (s), 619 (w).

2.4.2. $[(CuCN)_3L]_n$ (*2*)

The preparation of **2** is similar to that of **1** except that CuCN was used instead of AgCN and the reaction was carried out at 160 °C in ethanol. White prism crystals of **2** were obtained (19% yield based on CuCN). Anal. Calcd for $C_{37}H_{38}Cu_3N_{11}$ (827.43): C, 53.71; H, 4.63; N, 18.62. Found: C, 52.61; H, 4.32; N, 18.60. IR (cm^{-1}): 3119 m, 2986(w), 2116(s), 1620(w), 1508(s), 1474(m), 1396(w), 1296(w), 1224(s), 1109(s), 1084(s), 1023(w), 937(w), 817(m), 764(w), 742(m), 653(m), 612(w).

2.4.3. $[(AgSCN)_2L]_n$ (*3*)

Yellow prism crystals of **3** were obtained in a similar way as for 1 except that AgSCN was employed instead of AgCN and the reaction was carried out at 160 °C (yield: 59% based on AgSCN). Anal. calcd for $C_{36}H_{38}Ag_2N_{10}S_2$ (890.62): C, 48.55; H, 4.30; N, 15.73. Found: C, 48.98; H, 3.79; N, 15.65. IR (cm^{-1}): 3118 (m), 2925 (w), 2071 (s), 1631 (w), 1506 (m), 1384 (m), 1293 (w), 1229 (m), 1108 (m), 1084 (m), 1029 (w), 926 (w), 825 (w), 743 (w), 657 (w).

2.4.4. $[(CuSCN)_2L]_n$ (*4*)

White prism crystals of **4** were obtained by the similar method described for **3** except that CuSCN was used instead of AgSCN (about 61% yield based on CuSCN). Anal. Calc for $C_{36}H_{38}Cu_2N_{10}S_2$ (801.98): C, 53.92; H, 4.78; N, 17.47. Found: C, 53.01; H, 5.02; N, 17.60. IR (cm^{-1}): 3116(m), 2975(w), 2087(s), 1631(w), 1510(s), 1499(m). 1385(m), 1294(w), 1275(w), 1222(s), 1106(s), 1186(s), 1024(w), 924(w), 848(w), 827(m), 806(w), 759(m), 746(m), 658(m), 616(w).

Table 1
Crystallographic data and structure refinement summary for complexes **1**–**4**.

Complex	**1**	**2**	**3**	**4**
Chemical formula	$C_{37}H_{38}Ag_3N_{11}$	$C_{37}H_{38}Cu_3N_{11}$	$C_{36}H_{38}Ag_2N_{10}S_2$	$C_{36}H_{38}Cu_2N_{10}S_2$
Formula weight	960.39	827.43	890.64	802.00
Crystal system	Orthorhombic	Monoclinic	Monoclinic	Monoclinic
Space group	$Pna2_1$	$P2_1/c$	$P2_1/c$	$P2_1/c$
a (Å)	17.9554(6)	11.683(8)	18.931(3)	18.389(5)
b (Å)	12.6230(5)	12.680(8)	11.4590(19)	11.479(3)
c (Å)	16.6588(6)	25.831(18)	17.253(3)	16.992(4)
α (°)	90	90	90	90
β (°)	90	97.184(7)	95.592(3)	97.692(4)
γ (°)	90	90	90	90
V (Å^3)	3775.7(2)	3797(4)	3725.1(11)	3554.5(15)
Z	4	4	4	4
D (cal.)(mg m^{-3})	1.689	1.448	1.588	1.499
μ (mm^{-1})	1.583	1.707	1.205	1.357
F(000)	1912	1696	1800	1656
T (K)	293(2)	293(2)	293(2)	293(2)
R_1[a], $wR_2[I>2\sigma(I)]$[b]	0.0328, 0.0906	0.0878, 0.1607	0.0407, 0.1035	0.0577, 0.1424
Total/unique/*R*int	28219/7754/0.0189	28540/8706/0.0733	28617/8531/0.0207	27146/8136/0.0307

[a] $R_1 = \Sigma||F_o|-|F_c||/\Sigma|F_o|$.
[b] $wR2 = [\Sigma w(F_o^2 - F_c^2)^2/\Sigma w(F_o^2)^2]^{0.5}$.

2.5. X-ray crystallography

The X-ray single-crystal data of **1**–**4** are listed in Table 1. Intensity data were collected at room temperature on a Rigaku Mercury CCD area-detector diffractometer with a graphite-monochromator utilizing Mo$K\alpha$ radiation ($\lambda = 0.71073$ Å). Crystals of **1**–**4** suitable for X-ray crystallography were mounted on the top of a glass fiber with epoxy cement. The structure factors were obtained after Lorentz and polarization corrections. All non-hydrogen atoms were refined anisotropically. The structures were solved by direct methods and refined on F^2 by full-matrix least-squares using the SHELXL-97 program package. The organic hydrogen atoms were generated geometrically (C–H 0.96 Å).

Crystal data and details of the data collection and structure refinement are summarized in Table 1. Selected bond distances and angles for compounds **1**–**4** are listed in Table 2.

3. Results and discussion

3.1. Synthesis and general characterization

The ligand **L** was prepared as described in Scheme 1. It is soluble in common organic solvents such as CH_3OH, CH_3CN, $CHCl_3$, etc. Compounds **1**–**4** were prepared by the reactions of *M*CN or *M*SCN (*M* = Ag, Cu) with L in CH_3CN or EtOH under heating conditions. The IR spectra of **1**–**2** show characteristic CN groups at ca. 2120 cm^{-1} and those of **3**–**4** show SCN groups at ca. 2080 cm^{-1}. Other complicated peaks show the characteristic C–N and C–C vibrational frequencies for L ligands.

3.2. Crystal structures

3.2.1. $[(AgCN)_3L]_n$ (**1**)

The asymmetric unit of **1** contains three crystallographically independent Ag atoms, three cyanide groups and one L ligand. As shown in Fig. 1a, all the Ag atoms are in a nearly linear geometry with the C(1)–Ag(1)–N(4), N(10)–Ag(2)–N(8) and C(2)–Ag(3)–C(3)

Table 2
Selected bond distances (Å) and angles (°) for complexes **1**–**4**.

Complex **1**			
Ag(1)–C(1)	2.035(4)	Ag(1)–N(4)	2.117(3)
Ag(2)–N(8)	2.183(4)	Ag(2)–N(10)	2.162(4)
Ag(3)–C(2)	2.046(6)	Ag(3)–C(3)	2.054(5)
C(1)–Ag(1)–N(4)	170.56(16)	N(8)–Ag(2)–N(10)	171.74(11)
C(2)–Ag(3)–C(3)	175.7(3)		
Complex **2**			
Cu(1)–C(2)	1.851(6)	Cu(1)–N(1)	1.925(5)
Cu(1)–N(9)A	2.058(5)	Cu(2)–C(3)	1.929(5)
Cu(2)–N(2)	1.945(6)	Cu(2)–N(7)A	2.122(5)
Cu(2)–N(11)B	2.122(5)	Cu(3)–C(1)C	1.875(6)
Cu(3)–N(3)	1.903(6)	Cu(3)–N(5)	2.021(5)
C(2)–Cu(1)–N(1)	144.2(2)	C(2)–Cu(1)–N(9)A	119.3(2)
N(1)–Cu(1)–N(9)A	96.2(2)	C(3)–Cu(2)–N(2)	127.7(2)
C(3)–Cu(2)–N(7)A	110.7(2)	N(2)–Cu(2)–N(7)A	105.8(2)
C(3)–Cu(2)–N(11)B	102.2(2)	N(2)–Cu(2–N(11)B	107.3(2)
N(7)A–Cu(2)–N(11)B	99.69(19)	C(1)C–Cu(3)–N(3)	133.6(2)
C(1)C–Cu(3)–N(5)	108.1(2)	N(3)–Cu(3)–N(5)	118.0(2)
Complex **3**			
Ag(1)–N(4)	2.297(3)	Ag(1)–N(8)A	2.284(3)
Ag(1)–S(1)	2.7628(10)	Ag(1)–S(1)B	2.5452(9)
Ag(2)–N(2)C	2.300(3)	Ag(2)–N(6)D	2.315(3)
Ag(2)–N(10)	2.300(2)	Ag(2)–S(2)	2.6186(11)
N(4)–Ag(1)–N(8)A	102.10(10)	N(4)–Ag(1)–S(1)	102.93(7)
N(4)–Ag(1)–S(1)B	114.02(7)	N(8)A–Ag(1)–S(1)	104.72(8)
N(8)A–Ag(1)–S(1)B	124.66(9)	S(1)–Ag(1)–S(1)B	106.14(3)
N(2)C–Ag(2)–N(6)D	99.08(11)	N(2)C–Ag(2)–N(10)	126.25(12)
N(2)C–Ag(2)–S(2)	114.62(12)	N(6)D–Ag(2)–N(10)	107.51(10)
N(6)D–Ag(2)–S(2)	106.93(8)	N(10)–Ag(2)–S(2)	101.18(7)
Complex **4**			
Cu(1)–N(4)	2.029(3)	Cu(1)–N(8)A	2.035(3)
Cu(1)–S(1)	2.5099(13)	Cu(1)–S(1)B	2.3412(12)
Cu(2)–N(2)C	1.967(3)	Cu(2)–N(6)D	2.069(3)
Cu(2)–N(10)	2.007(3)	Cu(2)–S(2)	2.5607(13)
N(4)–Cu(1)–N(8)A	104.41(12)	N(4)–Cu(1)–S(1)	108.37(9)
N(4)–Cu(1)–S(1)B	115.89(8)	N(8)A–Cu(1)–S(1)	110.35(10)
N(8)A–Cu(1)–S(1)B	117.74(10)	S(1)–Cu(1)–S(1)B	99.84(4)
N(2)C–Cu(2)–N(6)D	98.25(13)	N(2)C–Cu(2)–N(10)	132.67(13)
N(2)C–Cu(2)–S(2)	108.57(13)	N(6)D–Cu(2)–N(10)	112.30(12)
N(6)D–Cu(2)–S(2)	99.94(10)	N(10)–Cu(2)–S(2)	100.96(9)

Symmetry code for **2**: A $-x, y-1/2, -z+1/2$; B $x-1, -y+5/2, z+1/2$; C $x, -y+5/2, z-1/2$; for **3** and **4**: A $-x, -y-1, -z+1$; B $-x,-y-1, -z$; C $-x-1, y+1/2, -z+3/2$; D $-x-1, -y-1, -z+1$.

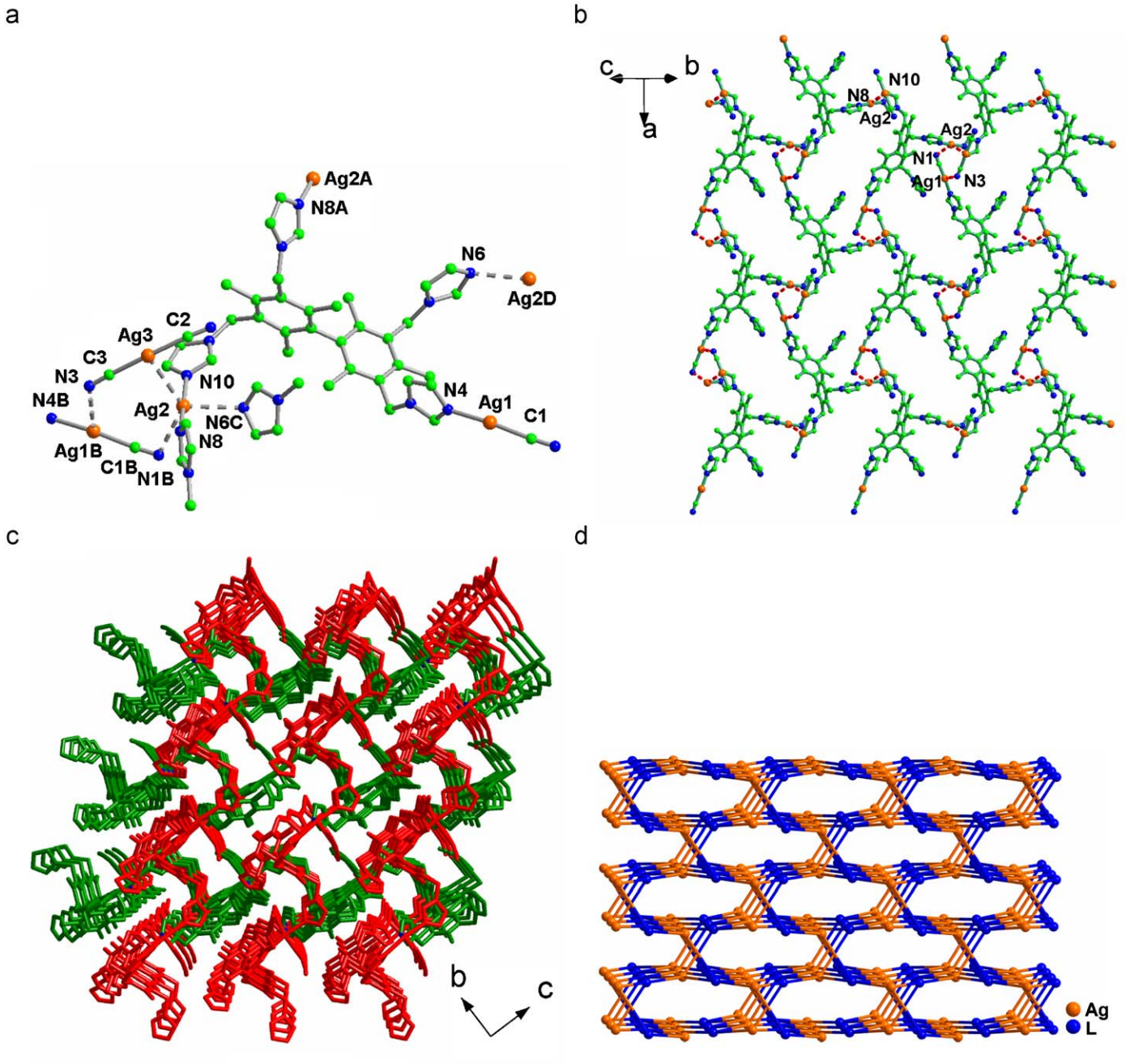

Fig. 1. (a) Environments of metal centers and L in **1**. Hydrogen atoms are omitted for clarity. Symmetry codes: (A) $-x+3/2, y-1/2, z-1/2$; (B) $1+x, y, z$; (C) $1-x, -y, 1/2+z$; (D) $1-x, -y, -1/2+z$; (b) view of the 2D sheet of **1** formed by 1D polymeric chains through the Ag–N(cyanide) weak interactions (the red dash lines stand for the weak interactions); (c) view of the 3D framework of **1** formed by Ag2–N6 weak interactions. (one stock of parallel layers is marked as red and the other as green) and (d) view of the topological representation of the uninodal 4-connected net of **1**. (For interpretation of the references to the color in this figure legend, the reader is referred to the web version of this article.)

angles of 170.56(16), 171.74(11) and 175.7(3)°, respectively. Each Ag(1) is bonded to one cyanide group and one N atom from one of the imidazole groups of L; each Ag(2) bridges two imidazole groups from different L ligands; whereas each Ag(3) is bonded to two cyanide groups. The Ag–N(L) and Ag–C(CN) bond lengths varying from 2.117(3) to 2.183(4) Å and 2.035(4) to 2.054(5) Å, respectively, are comparable with those for corresponding compounds [14,41–45]. The distance of Ag(2)–Ag(3) is 2.9517(4) Å, which is much shorter than twice of the van der Waals radii of silver atoms (3.4 Å) [46], indicating significant Ag–Ag interactions [47–50].

Complex **1** consists of a polymeric 1D chain formed through two imidazole groups of distinct L that is bridged by Ag(2). As seen in Fig. 1, although the N(3) atom of the terminal C(3)N(3) group is not coordinated to Ag(1B), the distance of Ag(1B)–N(3) (2.776 Å) is markedly shorter than the sum of the van der Waals radii of Ag and N atoms (3.27 Å) [46], suggesting a non-negligible interaction [19,48,51–63]. Similarly, Ag(2) also has a weak interaction with the N atom of the cyanide group attached to Ag(1) [Ag(2)–N(1B) = 2.675 Å], which links the adjacent 1D chains into an infinite 2D supramolecular sheet (Fig. 1b). Additionally, there exist weak interactions between Ag(2) and

the N atoms from the imidazole group of L [Ag(2)–N(6) = 2.677 Å] [51–64], which further extended the 2D sheets into a 3D supramolecular framework (Fig. 1c).

If Ag(3) atom is omitted due to its simply attribution to the framework, Ag(1) is treated as a 2-connected bridging , Ag(2) and L are both viewed as 4-connected nodes, the 3D supramolecular framework of **1** can be regarded as a new uninodal 4-connected net with Schläfli symbol is 6^6 and vertex symbol is $6.6.6^2.6^2.6^3.6^3$ (Fig. 1d), known to topos as a derived uninodal net and should be called sxa-4-*pbcn* as it is a 4-connected net derived from 6-connected sxa net descending in symmetry to *pbcn* [65].

3.2.2. $[(CuCN)_3L]_n$ (**2**)

Complex **2** crystallizes in the monoclinic space group $P2_1/c$. The asymmetric unit of **2** consists of three Cu atoms, three cyanide groups and one L ligand. As shown in Fig. 2a, there are two kinds of coordination geometry for the Cu atoms: Cu(1) and Cu(3) atoms are in an approximately trigonal environment, whereas Cu(2) lies in a distorted tetrahedral environment. The Cu(1) atom is coordinated by an imidazole N atom from the L ligand and two linear-bridged cyanide groups which subsequently bond to Cu(2) and Cu(3), respectively. The coordination environment of Cu(3) is similar to that of Cu(1). The coordination geometry at Cu(2) site is completed by two N donors from two L ligands and two linear-bridged cyanide groups which further link Cu(1) and Cu(3), respectively. The Cu(1), Cu(2) and Cu(3) atoms are linked in turn by the linear-bridged cyanide groups to form an 1D wave-like $[CuCN]_n$ chain. Such copper(I)–cyanide substructures are jointed together and extended to a 3D framework through L ligands (Fig. 2b).

As shown in Fig. 2c, a notable structural feature of **2** is that there exists a cube-like cage $\{Cu_4(CN)_2L_2\}$ which is constructed by four Cu atoms, two cyanide groups and two L ligands. Such cube-like units are connected to each other through Cu(3)–N(5) bonds and –Cu(3)–C(1)–N(1)–Cu(1)– edges to form a 1D chain, which has not been found previously for the metal complexes with imidazole-containing ligands (Fig. 2d).

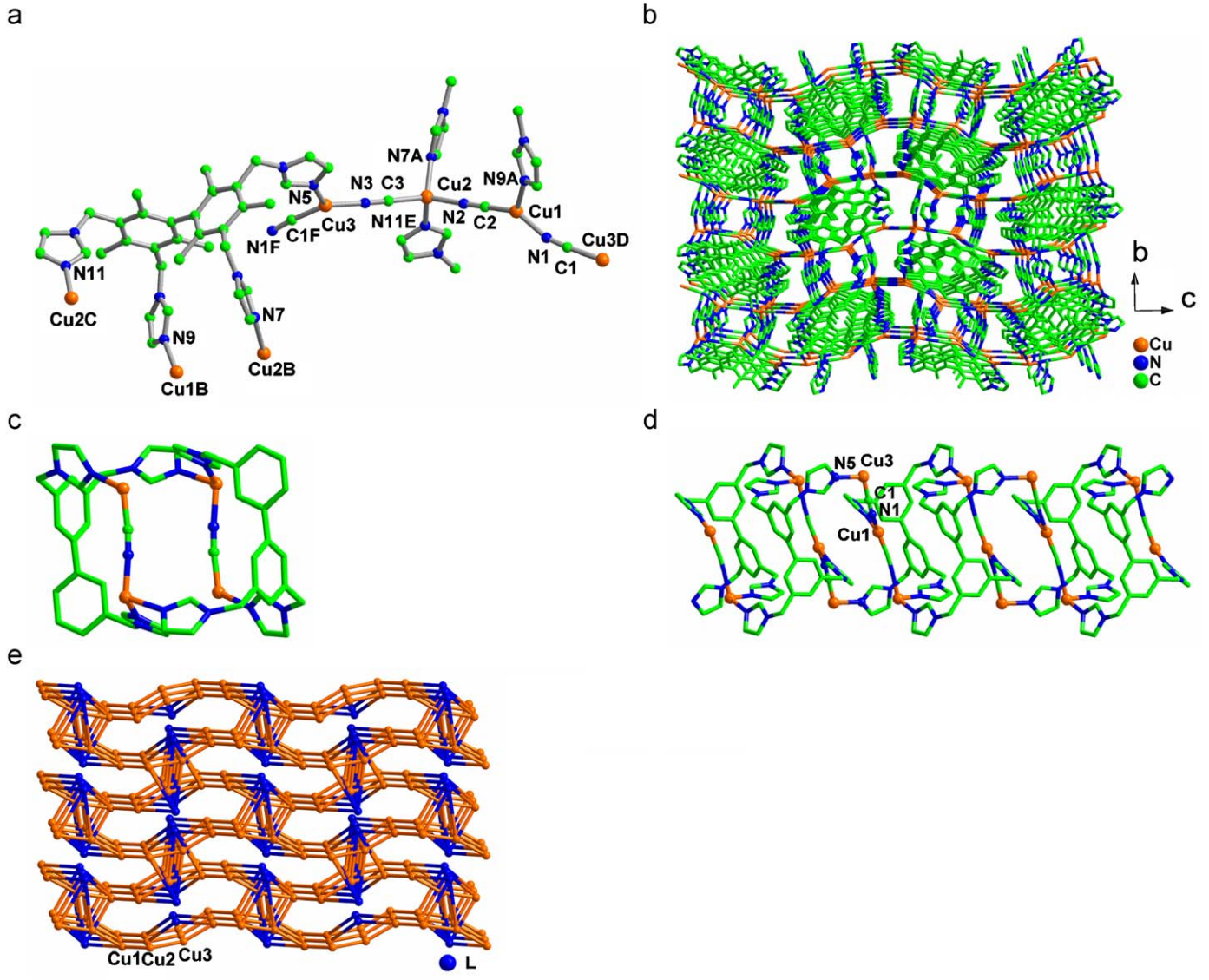

Fig. 2. (a) Environments of metal centers and L in **2**. Hydrogen atoms are omitted for clarity. Symmetry codes: (A) $-x$, $-1/2+y$, $1/2-z$; (B) $-x$, $1/2+y$, $1/2-z$; (C) $1+x$, $5/2-y$, $-1/2+z$; (D) x, $5/2-y$, $1/2+z$; (E) $-1+x$, $5/2-y$, $1/2+z$; (F) x, $5/2-y$, $-1/2+z$; (b) view of the 3D framework of **2**; (c) view of the single cube-like structure motif of **2**; (d) view of the chain structure in **2** constructed by cube-like cages; and (e) view of the topological representation of the tetranodal (3,4)-connected $(3\cdot4\cdot5\cdot10^2\cdot11)(3\cdot4\cdot5\cdot6\cdot7\cdot9)(3\cdot6\cdot7)(6\cdot10^2)$ framework of **2**.

From a topological perspective, the L ligand in **2** can also be view as four-connected node and the Cu(1)/Cu(2)/Cu(3) atom can be regarded as three/four/three-connected node. In this way, the structure of **2** could be rationalized as a tetranodal (3,4)-connected net. The molar ratio of these four kinds of nodes is 1:1:1:1. Thus, the framework of **2** is symbolized as a $(3\cdot4\cdot5\cdot10^2\cdot11)(3\cdot4\cdot5\cdot6\cdot7\cdot9)(3\cdot6\cdot7)(6\cdot10^2)$ network (Fig. 2e).

3.2.3. $[(AgSCN)_2L]_n$ (**3**)

X-ray crystal structure analyses reveal that the frameworks of **3** and **4** are isostructural and therefore only the structure of **3** is described in detail. As illustrated in Fig. 3a, there are two crystallgraphically independent silver(I) atoms in the crystal of **3**, and the stoichiometry for the silver(I) thiocyanate–L is 2:1. The Ag(1) atom displays a distorted tetrahedral coordination geometry comprised of two N atoms from two distinct L ligands [Ag(1)–N(4) = 2.297(3) and Ag(1)–N(8B) = 2.284(3) Å] and two different thiocyanate sulfur atoms [Ag(1)–S(1) = 2.7628(10) and Ag(1)–S(1A) = 2.5452(9) Å], with the angles varying from 102.10(10) to 124.66(9)°. The coordination environment of Ag(2) is also badly deviated from a tetrahedral geometry, surrounded by one N and one S atoms from two thiocyanate groups [Ag(2)–N(2D) = 2.300(3) and Ag(2)–S(2) = 2.6186(11) Å] and two N atoms from L [Ag(2)–N(10) = 2.300(2) and Ag(2)–N(6C) = 2.315(3) Å], with the angles ranging from 99.08(11)–126.25(12)°. The Ag–S bond lengths varying from 2.5452(9)–2.7628(10) Å are in the normal range found for the other siliver(I) thiocyanate complexes[19,66–70]. The distance between two Ag(1) atoms is 3.194(5) Å, which is a little longer than the similar distance in **1** but is still less than the sum of their van der Waals radii (3.4 Å) [46], indicating a weak metal–metal interaction.

In **3**, there exist two silver(I)–thiocyanate building blocks that serve as the polymeric links for the system. One is a four-membered symmetrical AgS_2Ag cyclic unit formed via two Ag(1) atoms and two bridging S-bonded thiocyanate ligands. The other is a $[AgSCN]_n$ zig-zag chain in which each thiocyanate ligand alternately connects two Ag(2) atoms through its S and N sites. As shown in Fig. 3b, the neighboring AgS_2Ag units are bridged by a pair of L ligands through N(4) and N(8), affording a 1D chain with 30-membered macrocycles. The remaining two imidazole N atoms [N(6) and N(10)] in each L are bonded to Ag(2) atoms of the $[AgSCN]_n$ zig-zag chains, giving rise to a 3D architecture (see Fig. 3c and Fig. S3).

Better insight into such a complicated framework can be accessed by the topology method. First, based on the consideration of their connectivity, both the Ag(1) atom and the AgS_2Ag parallelogram are viewed to be 4-connected nodes. Second, L can be simplified as a 4-connected node in the same way as for **1** and the thiocyanate groups are simplified to be linear connectors.

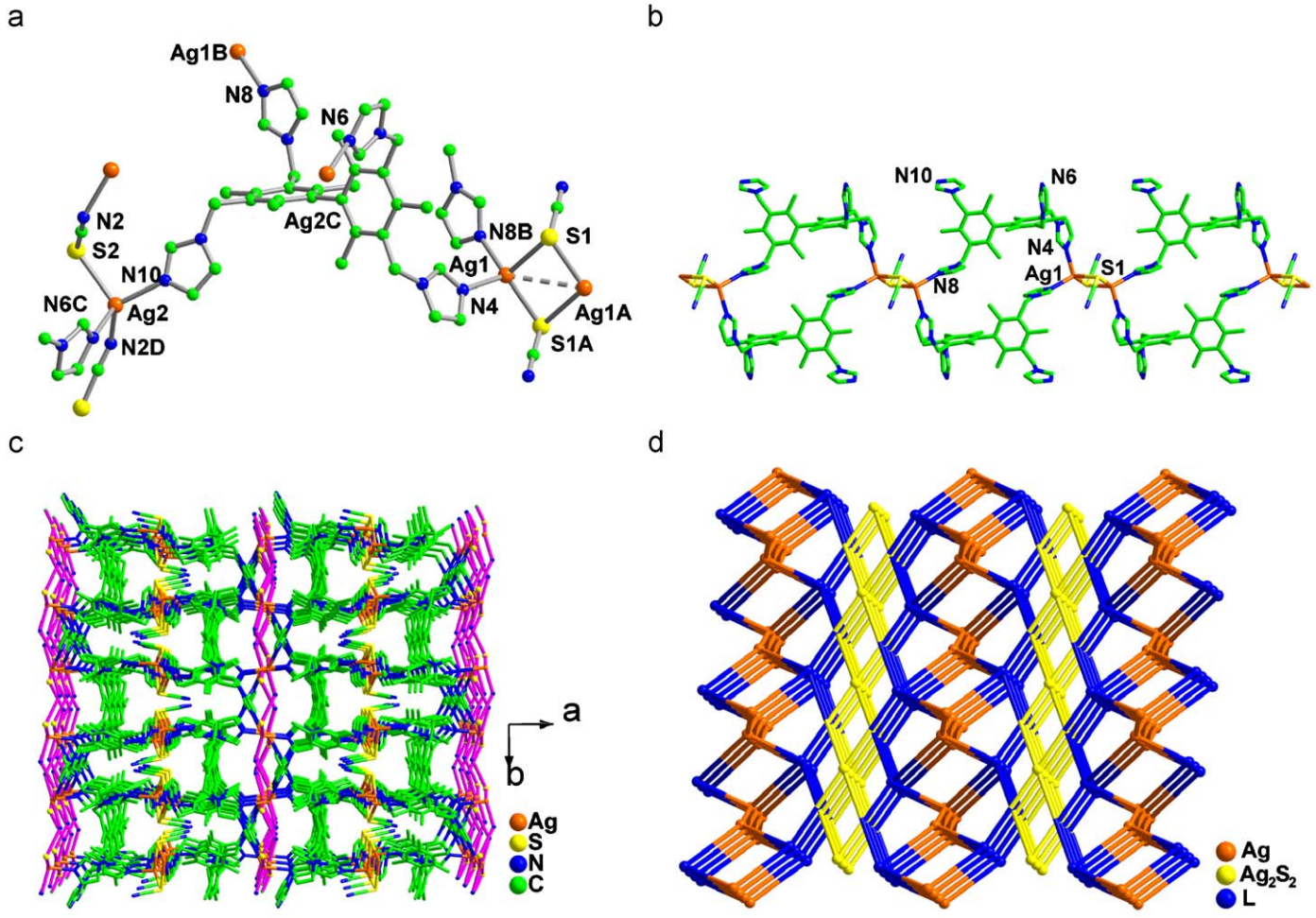

Fig. 3. (a) Environments of metal centers and L in **3**. Hydrogen atoms are omitted for clarity. Symmetry codes: (A) −*x*, −1−*y*, −*z*; (B) −*x*, −1−*y*, 1−*z*; (C) −1−*x*, −1−*y*, 1−*z*; (D) −1−*x*, 1/2+*y*, 3/2−*z*; (E) −1−*x*, −1/2+*y*, 3/2−*z*; (b) view of the 1D chain with 30-membered macrocycles in **3**; (c) view of the 3D framework of **3** (the $[AgSCN]_n$ zig-zag chain is marked as purple); (d) view of the topological representation of the 4-connected $(4\cdot8^5)_2(4^2\cdot8^2\cdot10^2)(4^2\cdot8^4)_2$ framework of **3** (the brown line stands for a SCN connector). (For interpretation of the references to the color in this figure legend, the reader is referred to the web version of this article.)

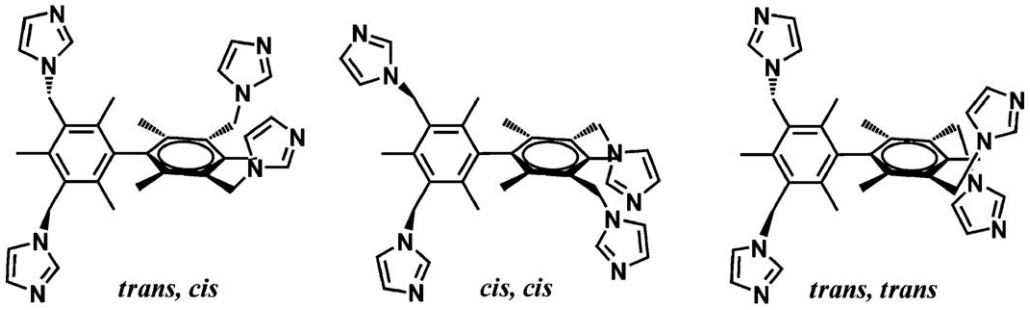

Chart 1. Different coordination conformations of L.

Therefore, the combination of nodes and connectors suggests a trinodal 4-connected net for the present case (Fig. 3d). The topological notation for such a 4-connected net is $(4\cdot8^5)_2(4^2\cdot8^2\cdot10^2)(4^2\cdot8^4)_2$.

As we can see in the structures of **1**–**4**, to minimize the steric repulsion arises from the neighboring methyl groups, the two benzene rings of L are almost perpendicular to each other with the dihedral angle between them varying from 80.3° to 86.4°. This can prevent the free rotation between the benzene rings and reduce the conformational flexibility of L. However, due to the existence of the flexible methylene groups, L can adopt several conformations depending on the orientation of its four imidazole arms (Chart 1), which will lead different structures. Based on one benzene ring, the relative orientation of the imidazole groups results in three overall conformations of L *viz.* (*trans*, *cis*), (*cis*, *cis*) and (*trans*, *trans*) as displayed in the structures of **1**, **2** and **3**, respectively. In the structure of **1**, the Ag(I) is two coordinated, and L takes a *trans*, *cis* conformation, whereas in **3**, the Ag(I) is four-coordinated and L adopts a *trans*, *cis* conformation. Different from that observed in **1** and **3**, the L ligand of **2** takes a *cis*, *cis* conformation so that the three imidazoles are oriented to the same direction and link three Cu(I) to give a novel cube-like $\{Cu_4(CN)_4L_2\}$ subunit.

3.3. Ferroelectric properties

Recently, a prevalent research have focused on developing ferroelectric materials based on metal-organic frameworks (MOF) and have reported some such materials [6,71,72]. However, the reported ferroelectric materials are mostly built upon chiral organic tectons, whereas the proper use of achiral ligands by spontaneous are scarce [17,71]. Herein, we describe the preliminary investigation of the possible ferroelectric property of complex **1**.

Complex **1** crystallizes in the noncentric space group $Pna2_1$, which belongs to the polar point group $C2v$, which falls in one of the 10 polar point groups ($C1$, Cs, $C2$, $C2v$, $C4$, $C4v$, $C3$, $C3v$, $C6$, $C6v$) required for ferroelectric materials. Therefore, the ferroelectric behavior of **1** was examined. Fig. 4 clearly shows that there is an electric hysteresis loop that is a typical ferroelectric feature with a remanent polarization (Pr) of ca. 0.026 μC cm^{-2} and coercive field (Ec) of ca. 800 V cm^{-1}. The saturation spontaneous polarization (Ps) of **1** is ca. 0.047 μC cm^{-2}. Furthermore, we also studied the behavior of permittivity $(\varepsilon)=\varepsilon_1(\omega)-i\varepsilon_2(\omega)$, where $\varepsilon_1(\omega)$ and $\varepsilon_2(\omega)$ are the real (dielectric constant) and imaginary (dielectric loss) parts, respectively. As shown in Fig. S4, the frequency dependence of the dielectric constant ε_1 at room temperature (20 °C) indicates that ε_1 rapidly decreases with the increase of frequency, while dielectric loss $\tan\delta$ remains unchanged.

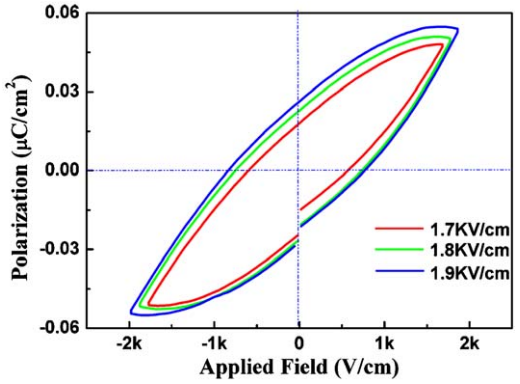

Fig. 4. Electric hysteresis loop of **1**, observed for a powdered sample in the form of a pellet on a ferroelectric.

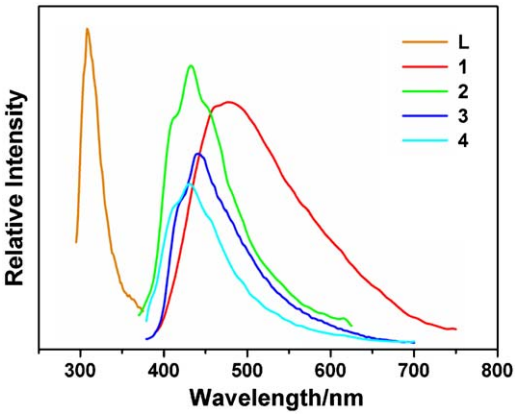

Fig. 5. Solid-state emission spectra for L and complexes **1**–**4** at room temperature.

3.4. Luminescent properties

The solid-state photoluminescent spectra of L and compounds **1**–**4** are depicted in Fig. 5. The free ligand exhibits a sharp and intense emission peak at 308 nm upon excitation at 283 nm, whereas compounds **1–4** display emissions at about 472 nm for **1** ($\lambda_{ex}=382$ nm), at 432 nm for **2** ($\lambda_{ex}=348$ nm), at 444 nm for **3** ($\lambda_{ex}=364$ nm) and 431 nm for **4** ($\lambda_{ex}=360$ nm). In comparison with the photoluminescence properties of reported complexes of silver/cuprous pseudohalides and heterocyclic ligands [19,21,37,73–75], we tentatively assigned the emission of **1**, **3** and **4** as being the coupling of a metal-to-ligand transition (MLCT) and a metal-centered (MC) transition modified by metal–metal interactions. The origin of the emission band of 2 may be attributed to a metal-to-ligand transition. In addition,

thermogravimetric analysis (see the supporting information, Fig. S2) reveal that **1–4** are stable up to 298, 345, 276 and 294, respectively. Then, these coordination polymers may be excellent candidates for potential photoactive materials because they are highly thermally stable.

4. Conclusions

In summary, we have successfully synthesized four novel metal-organic coordination polymers built upon MX (M = Ag, Cu; $X = CN^-$, SCN^-) and a new tetradentate ligand L. All these polymers possess 3D frameworks and show rich topological varieties. It is expected that the conformational flexibility of L may offer new possibilities to construct new types of topology networks. Further research work on exploring the formation of functional materials by the use of L is in progress.

5. Supplementary material

Crystallographic data for the four complexes in this paper have been deposited at the Cambridge Crystallographic data center, CCDC nos. 688334, 692300, 688335 and 692301 are for complexes **1–4**, respectively. These data can be obtained free of charge at http://www.ccdc.cam.ac.uk/conts/retrieving-.html (or from the Cambridge Crystallographic Data Center, 12 Union Road, Cambridge CB2 1EZ, UK; fax: (+44) 1223-336-033; e-mail: deposit@ccdc.cam.ac.uk).

Acknowledgments

This work was supported by the grants from the State Key Laboratory of Structural Chemistry, Fujian Institute of Research on the Structure of Matter, Chinese Academy of Sciences (CAS, SZD08002-2), National Basic Research Program of China (973 Program, 2007CB815306), the National Natural Science Foundation of China (20733003 and 20673117) and Knowledge Innovation Program of the Chinese Academy of Sciences for financial support.

Appendix A. Supplementary material

Supplementary data associated with this article can be found in the online version at doi:10.1016/j.jssc.2009.03.012.

References

[1] M. Eddaoudi, D.B. Moler, H.L. Li, B.L. Chen, T.M. Reineke, M. O'Keeffe, O.M. Yaghi, Acc. Chem. Res. 34 (2001) 319–330.
[2] R. Kitaura, K. Seki, G. Akiyama, S. Kitagawa, Angew. Chem. Int. Ed. 42 (2003) 428–431.
[3] U. Mueller, M. Schubert, F. Teich, H. Puetter, K. Schierle-Arndt, J. Pastré, J. Mater. Chem. 16 (2006) 626–636.
[4] M. Royzen, Z.H. Dai, J.W. Canary, J. Am. Chem. Soc. 127 (2005) 1612–1613.
[5] A.P. DeSilva, H.Q.N. Gunaratne, T. Gunnlaugsson, A.J.M. Huxley, C.P. McCoy, J.T. Rademacher, T.E. Rice, Chem. Rev. 97 (1997) 1515–1566.
[6] D.W. Fu, Y.M. Song, G.X. Wang, Q. Ye, R.G. Xiong, T. Akutagawa, T. Nakamura, P.W.H. Chan, S.D. Huang, J. Am. Chem. Soc. 129 (2007) 5346–5347.
[7] H.P. Jia, W. Li, Z.F. Ju, J. Zhang, Dalton Trans. (2007) 3699–3704.
[8] J.Z. Gu, W.G. Lu, L. Jiang, H.C. Zhou, T.B. Lu, Inorg. Chem. 46 (2007) 5835–5837.
[9] W. Zhao, J. Fan, T. Okamura, W.Y. Yin, N. Ueyame, Microporous Mesoporous Mater. 78 (2005) 265–279.
[10] L. Song, J.R. Li, P. Lin, Z.H. Li, T. Li, S.W. Du, X.T. Wu, Inorg. Chem. 45 (2006) 10155–10161.
[11] L. Zhang, X.Q. Lu, C.L. Chen, H.Y. Tan, H.X. Zhang, B.S. Kang, Cryst. Growth Des. 5 (2005) 283–287.
[12] B.F. Hoskins, R. Robson, D.A. Slizys, J. Am. Chem. Soc. 119 (1997) 2952–2953.
[13] C.Y. Su, Y.P. Cai, C.L. Chen, F. Lissner, B.S. Kang, W. Kaim, Angew. Chem. Int. Ed. 41 (2002) 3371–3375.
[14] W.Y. Sun, J. Fan, T.A. Okamura, J. Xie, K.B. Yu, N. Ueyama, Chem. Eur. J. 7 (2001) 2557–2562.
[15] J. Fan, L. Gan, H. Kawaguchi, W.Y. Sun, K.B. Yu, W.X. Tang, Chem. Eur. J. 9 (2003) 3965–3973.
[16] B.F. Hoskins, R. Robson, D.A. Slizys, Angew. Chem. Int. Ed. 36 (1997) 2752–2755.
[17] L. Song, S.W. Du, J.D. Lin, H. Zhou, T. Li, Cryst. Growth Des. 7 (2007) 2268–2271.
[18] J. Fan, B.E. Hanson, Inorg. Chem. 44 (2005) 6998–7008.
[19] J.D. Lin, Z.H. Li, J.R. Li, S.W. Du, Polyhedron 26 (2007) 107–114.
[20] Q.M. Wang, G.C. Guo, T.C.W. Mak, Chem. Commun. (1999) 1849–1850.
[21] X. Liu, G.C. Guo, M.L. Fu, X.H. Liu, M. S Wang, J.S. Huang, Inorg. Chem. 45 (2006) 3679–3685.
[22] C.J. Shorrock, B.Y. Xue, P.B. Kim, R.J. Batchelor, B.O. Patrick, D.B. Leznoff, Inorg. Chem. 41 (2002) 6743–6753.
[23] L. Hou, D. Li, W.J. Shi, Y.G. Yin, S.W. Ng, Inorg. Chem. 44 (2005) 7825–7832.
[24] V. Lippolis, A.J. Blake, P.A. Cooke, F. Isaia, W.S. Li, M. Schröder, Chem. Eur. J. 5 (1995) 1987–1991.
[25] R.Q. Fang, X.M. Zhang, Inorg. Chem. 45 (2006) 4801–4810.
[26] C.X. Ren, H.L. Zhu, G. Yang, X.M. Chen, Dalton Trans. (2001) 85–90.
[27] C.X. Ren, B.H. Ye, F. He, L. Cheng, X.M. Chen, Cryst. Eng. Commun. 6 (2004) 200–206.
[28] C.M. Hartshorn, P.J. Steel, Aust. J. Chem. 50 (1997) 1195–1198.
[29] S. Hu, A.J. Zhou, Y.H. Zhang, S. Ding, M.L. Tong, Cryst. Growth Des. 6 (2006) 2543–2550.
[30] X.M. Zhang, Z.M. Hao, H.S. Wu, Inorg. Chem. 44 (2005) 7301–7303.
[31] A.J. Blake, N.R. Brooks, N.R. Champness, M. Crew, L.R. Hanton, P. Hubberstey, S. Parsons, M. Schröder, Dalton Trans. (1999) 2813–2817.
[32] Z.M. Hao, X.M. Zhang, Cryst. Growth Des. 7 (2007) 64–68.
[33] R.J. Trovitch, R.S. Rarig, J.A. Zubieta, R.L. LaDuca, Acta Cryst. E 63 (2007) m339–m341.
[34] S.A. Barnett, A.J. Blake, N.R. Champness, C. Wilson, Chem. Commun. (2002) 1640–1641.
[35] W.R. Knapp, J.G. Thomas, D.P. Martin, M.A. Braverman, R.J. Trovitch, R.L. LaDuca, Z. Anorg. Allg. Chem. 633 (2007) 575–581.
[36] J.G. Ding, H.Y. Ge, Y.M. Zhang, B.L. Li, Y. Zhang, J. Mol. Struct. 782 (2006) 143–149.
[37] J.D. Lin, Z.H. Li, T. Li, J.R. Li, S.W. Du, Inorg. Chem. Commun. 9 (2006) 675–678.
[38] P. Kovacic, C. Wu, Sterically Hindered Aromat. Compd. 26 (1961) 759–762.
[39] A.W. Van der Made, R.H. Van der Made, J. Org. Chem. 58 (1993) 1262–1263.
[40] H.K. Liu, W.Y. Sun, H.L. Zhu, K.B. Yu, W.X. Tang, Inorg. Chim. Acta. 295 (1999) 129–135.
[41] H.K. Liu, J. Hu, T.W. Wang, X.L. Yu, J. Liu, B.S. Kang, Dalton. Trans. (2001) 3534–3540.
[42] C.Y. Li, C.S. Lin, J.R. Li, X.H. Bu, Cryst. Growth Des. 7 (2007) 286–295.
[43] V. Urban, T. Pretsch, H. Hartl, Angew. Chem. Int. Ed. 44 (2005) 2794–2797.
[44] W. Han, L. Yi, Z.Q. Liu, W. Gu, S.P. Yan, P. Cheng, D.Z. Liao, Z.H. Jiang, Eur. J. Inorg. Chem. (2004) 2130–2136.
[45] H. Zhang, J.W. Cai, X.L. Feng, T. Li, X.Y. Li, L.N. Ji, Inorg. Chem. Commun. 5 (2002) 637–641.
[46] A.J. Bondi, J. Phys. Chem. 68 (1964) 441–451.
[47] V. Niel, A.L. Thompson, A.E. Goeta, C. Enachescu, A. Hauser, A. Galet, M.C. Muñoz, J.A. Real, Chem. Eur. J. 11 (2005) 2047–2060.
[48] X. Liu, G.C. Guo, M.L. Fu, W.T. Chen, Z.J. Zhang, J.S. Huang, Dalton Trans. (2006) 884–886.
[49] M.A. Omary, T.R. Webb, Z. Assefa, G.E. Shankle, H.H. Patterson, Inorg. Chem. 37 (1998) 1380–1386.
[50] T. Dorn, K.M. Fromm, C. Janiak, Aust. J. Chem. 59 (2006) 22–25.
[51] S.R. Batten, B.F. Hoskins, R. Robson, New J. Chem. (1998) 173–175.
[52] C. Janiak, L. Uehlin, H.P. Wu, P. Klüfers, H. Piotrowski, T.G. Scharmann, Dalton Trans. (1999) 3121–3131.
[53] L. Carlucci, G. Ciani, P. Macchi, D.M. Proserpio, S. Rizzato, Chem. Eur. J. 5 (1999) 237–243.
[54] D. Fortin, M. Drouin, P.D. Harvey, F.G. Herring, D.A. Summers, R.C. Thompson, Inorg. Chem. 38 (1999) 1253–1260.
[55] K.E. Bessler, L.L. Romualdo, V.M. Deflon, A.Z. Hagenbach, Z. Anorg. Allg. Chem. 626 (2000) 1942–1945.
[56] C. Kleina, E. Graf, M.W. Hosseini, A. De Cian, J. Fischer, Chem. Commun. (2000) 239–240.
[57] J. Konnert, D. Britton, Inorg. Chem. 5 (1966) 1193–1196.
[58] M.A. Withersby, A.J. Blake, N.R. Champness, P. Hubberstey, W.S. Li, M. Schröder, Angew. Chem. Int. Ed. 36 (1997) 2327–2329.
[59] K. Nilsson, Å. Oskarsson, Acta Chem. Scand. A 38 (1984) 79–85.
[60] D.M. Barnhart, C.N. Caughlan, M. Ul-Haque, Inorg. Chem. 8 (1969) 2768–2770.
[61] G.A. Bowmaker, Effendy, P.C. Junk, A.H. White, Dalton Trans. (1998) 2131–2138.
[62] G.A. Bowmaker, Effendy, J.C. Reid, C.E.F. Rickard, B.W. Skelton, A.H. White, Dalton Trans. (1998) 2139–2146.
[63] C.J. Shorrock, B.Y. Xue, P.B. Kim, R.J. Batchelor, B.O. Patrick, D.B. Leznoff, Inorg. Chem. 4 (2002) 6743–6753.
[64] D.Z. Wang, C.S. Liu, J.R. Li, L. Li, Y.F. Zeng, X.H. Bu, Cryst. Eng. Commun. 9 (2007) 289–297.

[65] V.A. Blatov, Acta Cryst. A 63 (2006) 329–343.
[66] G.A. Bowmaker, E. endy, B.W. Skelton, A.H. White, Dalton Trans. (1998) 2123–2130.
[67] G.A. Bowmaker, E. endy, P.J. Harvey, P.C. Healy, B.W. Skelton, A.H. White, Dalton Trans. (1996) 2449–2457.
[68] C. Stockheim, K. Wieghardt, B. Nuber, J. Weiss, U. Flörke, H.-J. Haupt, Dalton Trans. (1991) 1487–1490.
[69] E. Bang, Acta Chem. Scand. 50 (1996) 952–953.
[70] Q.P. Hu, D.R. Chen, Y.D. Meng, Y.P. Fan, Jiegou Huaxue (J. Struct. Chem.) 14 (1995) 206–209.
[71] T. Okubo, R. Kawajiri, T. Mitani, T. Shimoda, J. Am. Chem. Soc. 127 (2005) 17598–17599.
[72] Q. Ye, Y.M. Song, G.X. Wang, K. Chen, D.W. Fu, P.W.H. Zhu, J.S. Chan, S.D. Huang, R.G. Xiong, J. Am. Chem. Soc. 128 (2006) 6554–6555.
[73] C.C. Wang, C.H. Yang, S.M. Tseng, S.Y. Lin, T.Y. Wu, M.R. Fuh, G.H. Lee, K.T. Wong, R.T. Chen, Y.M. Cheng, P.T. Chou, Inorg. Chem. 43 (2004) 4781–4783.
[74] X.Q. Wang, J.K. Cheng, Y.H. Wen, J. Zhang, Z.J. Li, Y.G. Yao, Inorg. Chem. Commun. 8 (2005) 897–899.
[75] L. Xi, G.C. Guo, M.L. Fu, W.T. Chen, Z.J. Zhang, J.S. Huang, Dalton Trans. (2006) 884–886.